

AD-A146 891

TWO-COLOR INTERFEROMETRIC LARGE-ANGLE ASTROMETRIC
OBSERVATIONS (U) MASSACHUSETTS INST OF TECH CAMBRIDGE
RESEARCH LAB OF ELECTRONICS M SHAO ET AL. 26 MAR 82

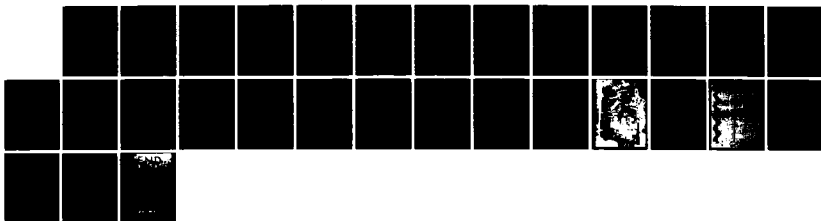
1/1

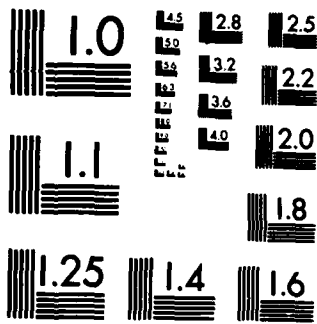
UNCLASSIFIED

N00014-80-C-0348

F/G 1777

NL





AD-A146 891

FINAL REPORT

United States Navy
Office of Naval Research
Contract N00014-80-C-0348

"Two-Color Interferometric
Large-Angle Astrometric Observations"

covering the period
April 1, 1980 - November 30, 1981

Michael Shao
David H. Staelin

March 26, 1982

Research Laboratory of Electronics
Massachusetts Institute of Technology
Cambridge, Massachusetts 02139

DTIC
OCT 20 1984

DTIC FILE COPY

84 10 19 127

UNCLASSIFIED

SECURITY CLASSIFICATION OF THIS PAGE (When Data Entered)

REPORT DOCUMENTATION PAGE		READ INSTRUCTIONS BEFORE COMPLETING FORM
1. REPORT NUMBER	2. GOVT ACCESSION NO.	3. RECIPIENT'S CATALOG NUMBER
	AD-A146891	
4. TITLE (and Subtitle) TWO-COLOR INTERFEROMETRIC LARGE-ANGLE ASTROMETRIC OBSERVATIONS		5. TYPE OF REPORT & PERIOD COVERED FINAL 4/1/80 - 11/30/81
		6. PERFORMING ORG. REPORT NUMBER
7. AUTHOR(s) Michael Shao and David H. Staelin		8. CONTRACT OR GRANT NUMBER(s) Contract N00014-80-C- 0348
9. PERFORMING ORGANIZATION NAME AND ADDRESS Research Laboratory of Electronics Massachusetts Institute of Technology Cambridge, Massachusetts 02139		10. PROGRAM ELEMENT, PROJECT, TASK AREA & WORK UNIT NUMBERS
11. CONTROLLING OFFICE NAME AND ADDRESS Department of the Navy Office of Naval Research Physics Program, Code 421		12. REPORT DATE March 26, 1982
		13. NUMBER OF PAGES
14. MONITORING AGENCY NAME & ADDRESS (if different from Controlling Office)		15. SECURITY CLASS. (of this report) Unclassified
		15a. DECLASSIFICATION/DOWNGRADING SCHEDULE
16. DISTRIBUTION STATEMENT (of this Report) Approved for public release; distribution unlimited.		
17. DISTRIBUTION STATEMENT (of the abstract entered in Block 20, if different from Report)		
18. SUPPLEMENTARY NOTES		
19. KEY WORDS (Continue on reverse side if necessary and identify by block number) Astrometric Interferometer Interferometer, Astrometric Star positions Instrument		
20. ABSTRACT (Continue on reverse side if necessary and identify by block number) Navigation depends upon position measurements of reference points such as stars, and system performance can be limited by the accuracy of the reference star coordinates. Under this program a dual-beam two-color astrometric interferometer was modified to permit large-angle differential astrometric observations. Stars separated 10-15 ^{deg} were to be observed with day-to-day repeatability of < 0.1 arc sec, with a goal of 0.02 arc sec		

UNCLASSIFIED

SECURITY CLASSIFICATION OF THIS PAGE (When Data Entered)

20. ABSTRACT (continued)

in declination. The initial system was installed at Mount Wilson in the fall of 1981 with a 3.4-meter N-S baseline and 5-cm light-collecting apertures. Initial tests revealed significant seismic noise at the site and refractive turbulence in the horizontal light beams. These and lesser problems are being solved, and successful operation in the spring of 1982 is anticipated. ↗

Accession For

DDA&I	<input checked="" type="checkbox"/>
DB	<input type="checkbox"/>
ed	<input type="checkbox"/>
on	
/	
ny Codes	
and/or	
erial	

AI

SUMMARY

Under this program a dual-beam two-color astrometric interferometer was modified to permit large-angle differential astrometric observations. Stars separated $10-15^\circ$ were to be observed with day-to-day repeatability of < 0.1 arc sec, with a goal of 0.02 arc sec in declination. The initial system was installed at Mount Wilson in the fall of 1981 with a 3.4-meter N-S baseline and 5-cm light-collecting apertures. Initial tests revealed significant seismic noise at the site and refractive turbulence in the horizontal light beams. These and lesser problems are being solved, and successful operation in the spring of 1982 is anticipated.

DISCUSSION

The instrument incorporates several novel features. In addition to the two-color fringe-tracking optics and the star trackers, there is a laser servo that controls the position of the delay line, and a large vacuum delay line that compensates for atmospheric dispersion.

The laser measures the position of each delay line with an rms error of $\sim 15 \text{ \AA}$, and the delay line length is then controlled with $\sim 100 \text{ \AA}$ precision. In this way errors in the delay line length introduced by the piezoelectric stack, voice coil, and stepping-motor translation unit are compensated, as is much of the seismic noise.

Measurements show that the seismic noise is dominated by a combination of 60 Hz, 50 Hz, and occasional random

signals. The 50- and 60-Hz signals together have an rms displacement of $\sim 250 \text{ \AA}$ and reduce fringe visibility. The 50-Hz signal appears to originate in the disk memory unit of the computer, which can be better isolated, and the 60-Hz signals have an unknown origin, but motors elsewhere on the Mount Wilson site are likely sources. This 50- and 60-Hz noise is being reduced by altering the resonant frequencies of excessively responsive optical components and by damping them. A separate trailer to house the computer is being sought too. This noise now degrades performance but does not terminate it. The random noise bursts have an unknown source but could originate at considerable distances.

The vacuum tanks are important to ensure that both paths between the star and the white fringe are equal and also that both paths pass through equal air masses. Equality of air masses is important because the atmosphere is dispersive, and inequality smears the fringes. Although this problem is compensated by a wedge of glass in some interferometers, the dispersive characteristics of glass are not adequate for these long baselines and wide spectral windows, which are approximately half an octave. Equality of air masses also removes the absolute errors due to the unknown refraction angle of the atmosphere, which is essential for precise large-angle astrometry.

The vacuum tanks also reduce the vulnerability of the instrument to local atmospheric turbulence, which is presently

significant because of the very cold weather relative to the warmth of the computer and other equipment residing in the shed with the interferometer optics. A partition between the computer and the optics was installed, and insulation of the optical table and large metallic components is underway.

The fluid level for monitoring table tilt was originally to contain mercury, but problems with the response time of mercury flowing in the interconnecting tube, the hazards and thermal expansion of mercury, and the ripples in the surface of the mercury have all forced a redesign of this system. Now salt water near the neutral thermal expansion point will be used together with appropriate fluid damping techniques. A large connecting tube will decrease the response time and help ensure homogeneity of the circulating solution.

Initial large-angle observations will be of stars brighter than \sim magnitude 3, and will involve a single two-color interferometer. They should commence at Mount Wilson in the late spring and summer of 1982 once the interferometer successfully tracks stellar fringes.

First fringe measurements with a
phase tracking stellar interferometer

Michael Shao
and
David H. Staelin

Research Laboratory of Electronics
Massachusetts Institute of Technology
Cambridge, Massachusetts 02139

ABSTRACT

A prototype two-telescope stellar interferometer with a 1.5 meter baseline has been used to track the white light fringes, 0.4 to 0.9 μ , from Polaris. Continuous fringe phase and amplitude measurements were made with \sim 220 photons per 4 msec integration time and 1.27 cm² collecting area under 2 arc sec seeing conditions. The same control algorithm should be able to track fringes from an 8.7 mag star using the light from two 5-inch telescopes and a 10 msec integration time under 1 arc sec seeing conditions. When tracking, the servo maintained equal path lengths to 0.1 μ rms in the two arms of the interferometer, thus cancelling the path length variations caused by earth rotation and atmospheric turbulence. In the future, two-color phase measurements will make optical aperture synthesis and optical VLBI astrometry possible.

I. INTRODUCTION

In recent years there has been considerable interest in very high angular resolution instruments, and several two-telescope stellar interferometers have been or are being built.¹⁻⁴ Most of these instruments were designed for stellar diameter or double star measurements, although in some cases aperture synthesis and astrometry are also possible. This paper describes the operation of a prototype interferometer⁵ that measures both fringe amplitude and phase at visible wavelengths; it has significant advantages over other approaches for several applications.

Several types of interferometers have been proposed for astrometry. These instruments can be categorized by two criteria. One criterion is whether they use a single color or two color fringe measurements. The second criterion is whether fringe phase or fringe amplitude is used to determine fringe position.

Single color interferometry in the infrared has been proposed for astrometry.⁴ However, the accuracy of single colors is ultimately limited by atmospheric effects. Although a long-baseline interferometer has an astrometric advantage over a conventional telescope,

this advantage surprisingly is not large. Quantitatively, the advantage depends on the power spectrum of phase fluctuations caused by the atmosphere. For a Kolmogorov spectrum, a 50 meter interferometer is only ~ 2 times more accurate than a 1 meter telescope; the standard deviation of the effective angle of arrival decreases only as the one-sixth power of the baseline length; while this is perhaps overly pessimistic, significant increases in accuracies are not to be expected.

The two-color technique⁵ can in principle eliminate astrometric errors caused by the atmosphere. The accuracy of a two-color instrument is limited by diffraction, photon noise, and systematic errors rather than by the atmosphere, and therefore significant improvement over the atmospheric limit is possible with long-baseline interferometers. However, atmospheric dispersion, which is necessary for the two-color technique to succeed, is significant only in the visible portion of the spectrum, and furthermore, the two-color technique is most effective only if one of the two colors is blue.

The second criterion is the method of measuring fringe position. Fringe envelope position measurements

have been proposed for an amplitude interferometer.¹ Fringe phase measurements can also be used for astrometry. The advantage of phase measurements is that they are generally much more accurate than fringe envelope measurements. The fringe envelope is wider than a single fringe by a factor of $\sim \lambda/\Delta\lambda$. In addition a wideband fringe tracker collects more photons by a factor of $\sim \lambda/\Delta\lambda$. The error due to photon noise is then smaller by $(\lambda/\Delta\lambda)^{1/2}$ for a tracker. The difference between a 100 Å bandwidth amplitude interferometer¹ and an octave bandwidth phase tracking interferometer is therefore a factor of $(\lambda/\Delta\lambda)^{3/2} \approx 350$ in accuracy or a factor of 10^5 in integration time.

These are the principal reasons for selecting a long-baseline stellar interferometer configuration that can measure fringe phase as well as amplitude.

Future versions of a two-color fringe tracking astrometric interferometer should be able to measure angular separations of stars to 10^{-4} arc sec accuracy over a 1 degree field of view with less than 1 hour of integration per star.⁵ Such an instrument would be able to detect a Sun-Jupiter System at 10 pc at the 10σ level and extend the direct calibration of the cosmic distance scale by one to two orders of magnitude.

II. THE INSTRUMENT

The prototype interferometer, Fig. 1, consists of three subsystems: the star trackers, the fringe tracker, and the laser interferometer which monitors the position of the optics.

Starlight from two alt-AZ siderostats 1.5 meters apart is combined at a beam splitter; the interfering wave fronts are kept parallel by star trackers in each arm. The two-inch beam from each siderostat is split by an annular mirror and directed into a star tracker and the beam splitter, as shown in Fig. 2. Each star-tracker error sensor consists of a telescope with a four-sided pyramid at the focal plane followed by four phototubes interfaced to a minicomputer. The computer corrects for differences in dark count and quantum efficiencies of the phototubes.

The fringe tracker uses a path length modulation technique, described later, to measure fringe position. This fringe position is then used to control the optical delay line so that the fringe is "tracked." The operation of the fringe tracker is very similar to certain other active optical systems that follow the phase fluctuations caused by atmospheric turbulence^{6,7}.

The prototype stellar interferometer uses a path length modulation technique for fringe detection. The path length in one arm of the interferometer is changed in a triangle wave pattern at 500 Hz with a one-wavelength peak-to-peak amplitude. Each sweep of the mirror is divided into four equal intervals. The number of photons detected in each of these intervals, i.e., A, B, C, and D, is used to estimate the fringe phase.

$$\phi = \tan^{-1}[(A - C)/(B - D)]. \quad (1)$$

The rms error in fringe phase due to photon noise is:

$$\Delta\phi = \left(\frac{1}{V} \frac{\pi}{2}\right)^{\frac{1}{2}}, \quad (2)$$

where N is the total number of detected photons and V is the apparent fringe visibility, which is a function of spatial coherence, temporal coherence and scintillation.

In the prototype interferometer, the phase ϕ was measured on a time scale τ sufficiently short to freeze the atmosphere; τ was a variable in the fringe demodulation subroutine. The estimated value ϕ was used as the input to a digital low pass filter, the output of

which was used to control the voltage to a piezo-electric transducer. The mirror mounted on the piezoelectric ceramic was the high-speed, high-resolution part of a three-stage optical delay line. The second stage was a voice-coil driven mirror. The third stage was a motor-driven translation stage. The voice coil was servoed to the piezoelectric transducer, i.e., the voice coil was moved such that if the piezoelectric transducer had been moved to its null position, the total optical delay would have remained constant. Similarly the translation stage was servoed to the voice coil. All the motors, transducers, etc. were directly interfaced to the computer and all the servoes were implemented in software.

As was explained earlier, it is necessary for a long-baseline interferometer to first find the fringe before tracking it. This is done by monitoring a variable Q , defined by Eq. (3),

$$Q = [(A - C)^2 + (B - D)^2] / (A + B + C + D), \quad (3)$$

where A , B , C , and D are photon counts used in Eq. (1). In the limit of large photon counts, Q is proportional to the square of the fringe amplitude signal-to-noise ratio. In the absence of fringes, Q has a mean value of 1.

The fringe amplitude monitor calculates Q every τ msec, when phase ϕ is calculated. From the current and previous values of Q , the fringe amplitude monitor switches the servo on or off and indicates to the observer whether or not the fringes have been found.

Several fringe amplitude monitor algorithms were tested, via both Monte-Carlo simulation and hardware. The algorithm used in the prototype, while not optimal in any sense, was quite adequate. The monitor can be in one of three states: fringes not found, fringes found and tracked, and fringes maybe. Transitions between these states are determined by the current value of Q and the value of Q that has been filtered with a low pass filter. This algorithm can respond quickly to turn the servo on before temporal coherence is lost due to fringe motion but is quite insensitive to noise that would accidentally turn the servo off when the fringe is being tracked.

III. OPERATION OF THE PROTOTYPE AT MOUNT WILSON

The prototype interferometer was used to track the white light fringe from Polaris on several nights in the early part of March 1979. Most of the data reported in this paper was obtained on March 7, 1979. Effective aperture of the interferometer was 1.27 cm^2 .

Table I lists the relevant parameters for the experiment.

For an interferometer with two 5-inch apertures, the total collecting aperture would be 253 cm^2 . This size aperture is possible if high-speed star trackers are used for guiding. If we also assume that 10-msec integration times are possible, the limiting magnitude is $2.5 \times \log(253 \times 2.5/1.27) + 2.0 = 8.7 \text{ mag}$. At Mount Wilson, Polaris is at a zenith angle of $\sim 56^\circ$, corresponding to 1.8 air mass. Under normal conditions, a stellar interferometer would limit itself to stars within $\sim 30^\circ$ zenith angle, 1.15 air mass, in order to minimize dispersive image spreading. Therefore, the seeing conditions for which the current fringe-tracking algorithm would track 8.7 mag stars with 5-inch optics are not exceptional conditions for a site such as Mount Wilson.

The fringe-finding algorithm had no trouble finding the fringe with 220 photons/4 msec. While the seeing was quite good for most of the night of 3 March 1979, there were times when the seeing would deteriorate to $\sim 4 \text{ arc sec}$. At these times, the fringe finder could still reliably find the fringe although the tracker would not be able to track the fringe for more

than a few seconds at a time. With a 4-msec integration time the fringe finder would search for the fringe by sweeping the optical delay lines at $62\lambda/\text{sec}$.

The fringe tracker could typically track the fringe motion caused by turbulence for several minutes before losing the fringe. A fringe recovery algorithm, which was not optimized, took 2-10 sec to reacquire the white light fringe. Figure 3 is a picture of a typical fringe. The scope trace was generated by the computer. Photon events were counted in 250 μsec bins and then displayed on the scope via a D/A converter. The quantization in Fig. 3 corresponds to 1 photon. In the laboratory, reliable servo operation was possible with a photon flux of 80 photons/ τ msec. In theory, fringe tracking is possible with ~ 30 photons/ τ msec. The current fringe tracking algorithm is ~ 2 stellar magnitudes from the theoretical limit for this type of servo.

Figure 4 shows the fringe motion, caused by the atmosphere, and the servo error. One quantity of interest is the mean square phase motion σ_{ϕ}^2 caused by atmospheric turbulence:

$$\sigma_{\phi}^2(\tau) \triangleq \langle [\phi(t) - \phi(t + \tau)]^2 \rangle, \quad (4)$$

where $\phi(t)$ is the fringe position as a function of time and $\langle \rangle$ denotes ensemble average. σ_ϕ^2 can be related to the phase structure function by Taylor's hypothesis. For Kolmogorov turbulence, σ_ϕ^2 should exhibit a $\tau^{5/3}$ dependence. Our data shows a $\tau^{4/3}$ dependence. A departure from Kolmogorov turbulence may be due to the fact that the interferometer was only ~ 1 meter from the ground and the outer scale of turbulence was not significantly larger than the 1.5 meter baseline of the interferometer. Departures from the $\tau^{5/3}$ dependence have also been reported elsewhere.⁹ In Fig. 5 we see the curve rolling off for large τ ; this is expected when the wind speed V times the lag τ is greater than 1.5 meters.

An additional improvement of $\sqrt{3.4}$ in signal-to-noise ratio, or 1.33 mag, is expected if a fringe detector that estimates both fringe phase and fringe velocity is used.¹⁰ In other words, fringe tracking of 10-mag stars should be possible.

IV. CONCLUSIONS

We have demonstrated the operation of a fringe tracking two-telescope interferometer on Polaris for 2 arc sec seeing. Our preliminary measurements show that 8.7 to 10 mag stars should be observable with

two 5-inch telescopes. The sensitivity of fringe-tracking interferometers compares favorably with the sensitivity of other types of long-baseline interferometers, even those with much larger apertures.

ACKNOWLEDGMENT

This work was supported by the National Science Foundation under Grant AST77-06052 A01 and by the M.I.T. Sloan Fund for Basic Research.

References

1. K. Liewer, "The prototype very long baseline amplitude interferometer" (IAU Coll. #50), Ed. J. Davis and W. Tango, E-1, 1978.
2. A. Labeyrie, "Interference fringes obtained on Vega with two optical telescopes," *Astrophys. J. Lett.* Ed. 196, L71-75 (1 March 1975).
3. J. Davis, "A prototype 11 meter modern Michelson stellar interferometer" (IAU Coll. #50), 14-1, 1978.
4. J. Storey, "The potential for astrometry in the infrared" (IAU Coll. #50), 20-1, 1978.
5. M. Shao and D. H. Staelin, "Long-baseline optical interferometer for astrometry," *J. Opt. Soc. Am.* 67, 81-86 (1977).
6. S. L. McCall et al., "Improved optical stellar image using a real-time phase-correction system: initial results," *Astrophys. J.* 211, 463-468 (15 Jan. 1977).
7. A. Buffington et al., "Correction of atmospheric distortion with an image-sharpening telescope," *J. Opt. Soc. Am.* 67, 298-303 (1977).
8. R. H. Hudgin, "Wave-front reconstruction for compensated imaging," *J. Opt. Soc. Am.* 67, 375-378 (1977).

9. R. J. Hill and S. F. Clifford, "Modified spectrum of atmospheric temperature fluctuations and its application to optical propagation," J. Opt. Soc. Am. 68, 892-899 (1978).
10. D. L. Fried, "Statistics of a geometric representation of wavefront distortion," J. Opt. Soc. Am. 55, 1427-1435 (1965).

Figure Captions

FIG. 1. Prototype stellar interferometer. Star tracker sensors are clusters of four tubes; piezo-controlled primary mirrors are at ends; main phototubes are large, rectangular, and near upper right; voice coil translator stage is at center left.

FIG. 2. Optical schematic of star trackers.

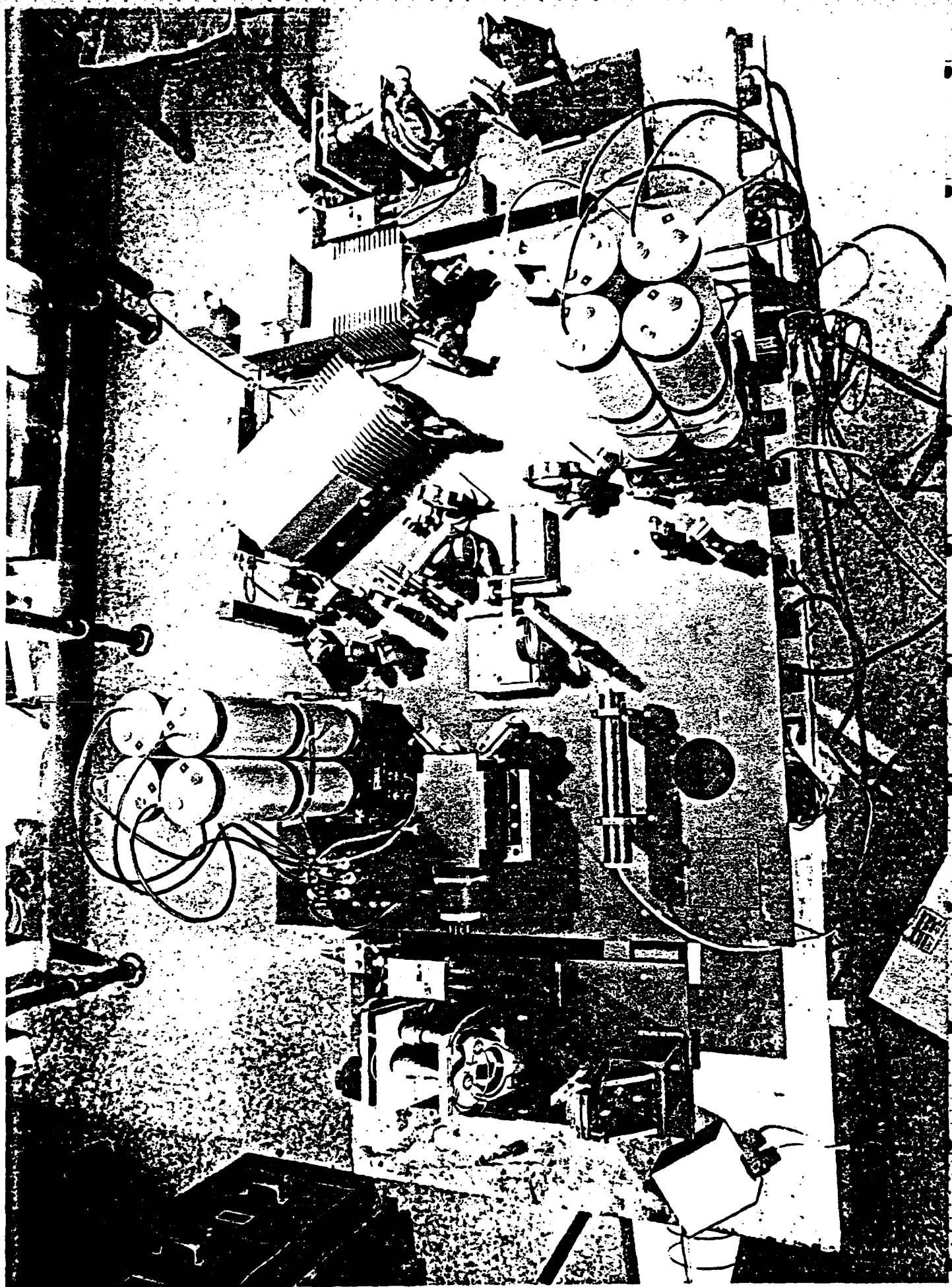
FIG. 3. Fringe detector phototube output.

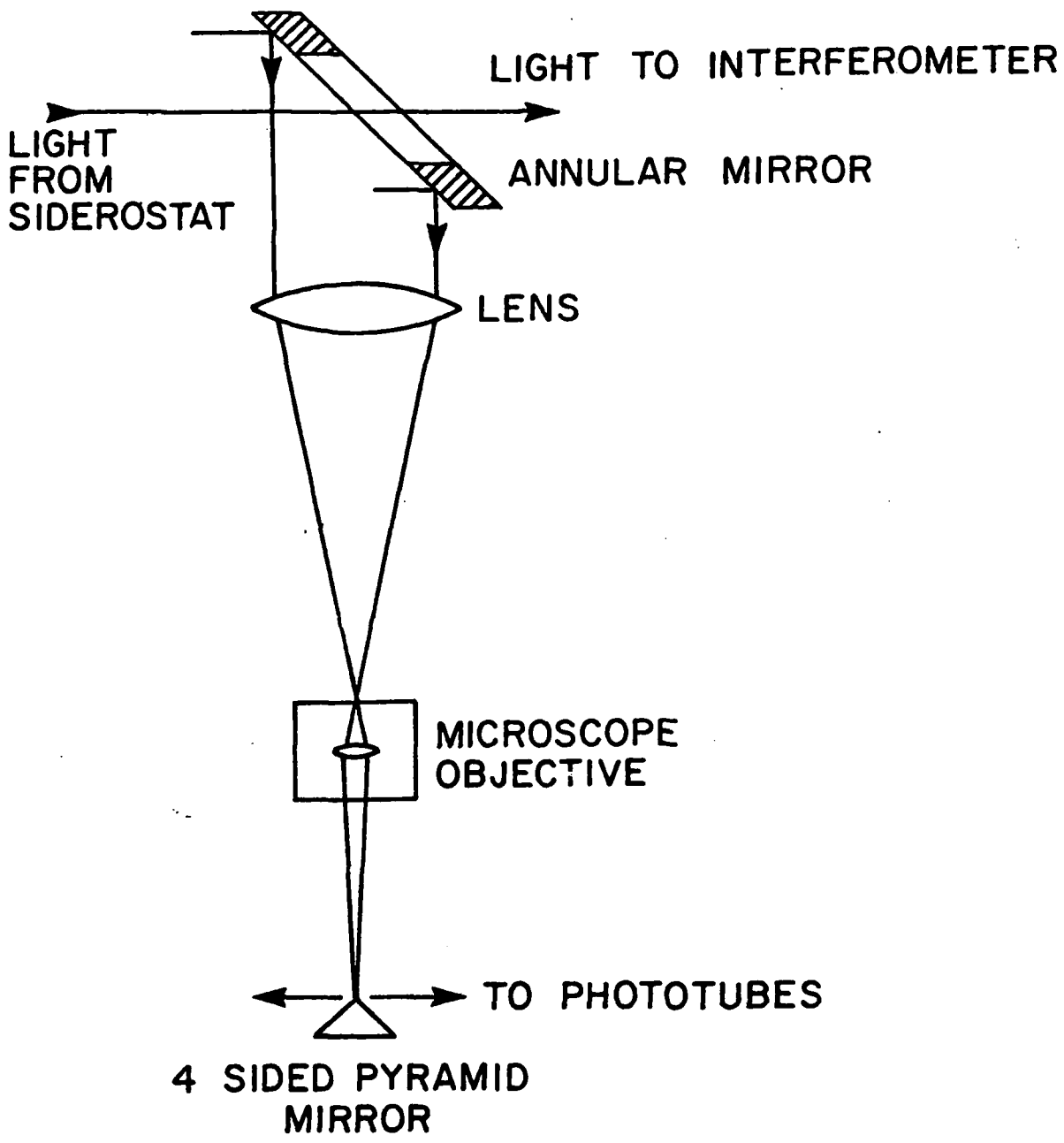
FIG. 4. Fringe motion due to turbulence.

FIG. 5. Mean square fringe motion vs. time lag.

Table I. Experiment Summary

seeing/ r_0	2 arc sec/5 cm
τ_0	4 msec
aperture area	1.27 cm ²
baseline	1.5 meters
photon flux	220 detected photons/4 msec from Polaris
rms servo error	0.1 μ
rms fringe velocity	13 μ /sec (due to turbulence)
fringe motion due to earth rotation	1.6 μ /sec
P-P fringe motion in \sim 4 sec (atmosphere, earth rotation)	7.6 μ
optical bandwidth	0.4 μ to 0.9 μ (GaAs phototube, no filter)

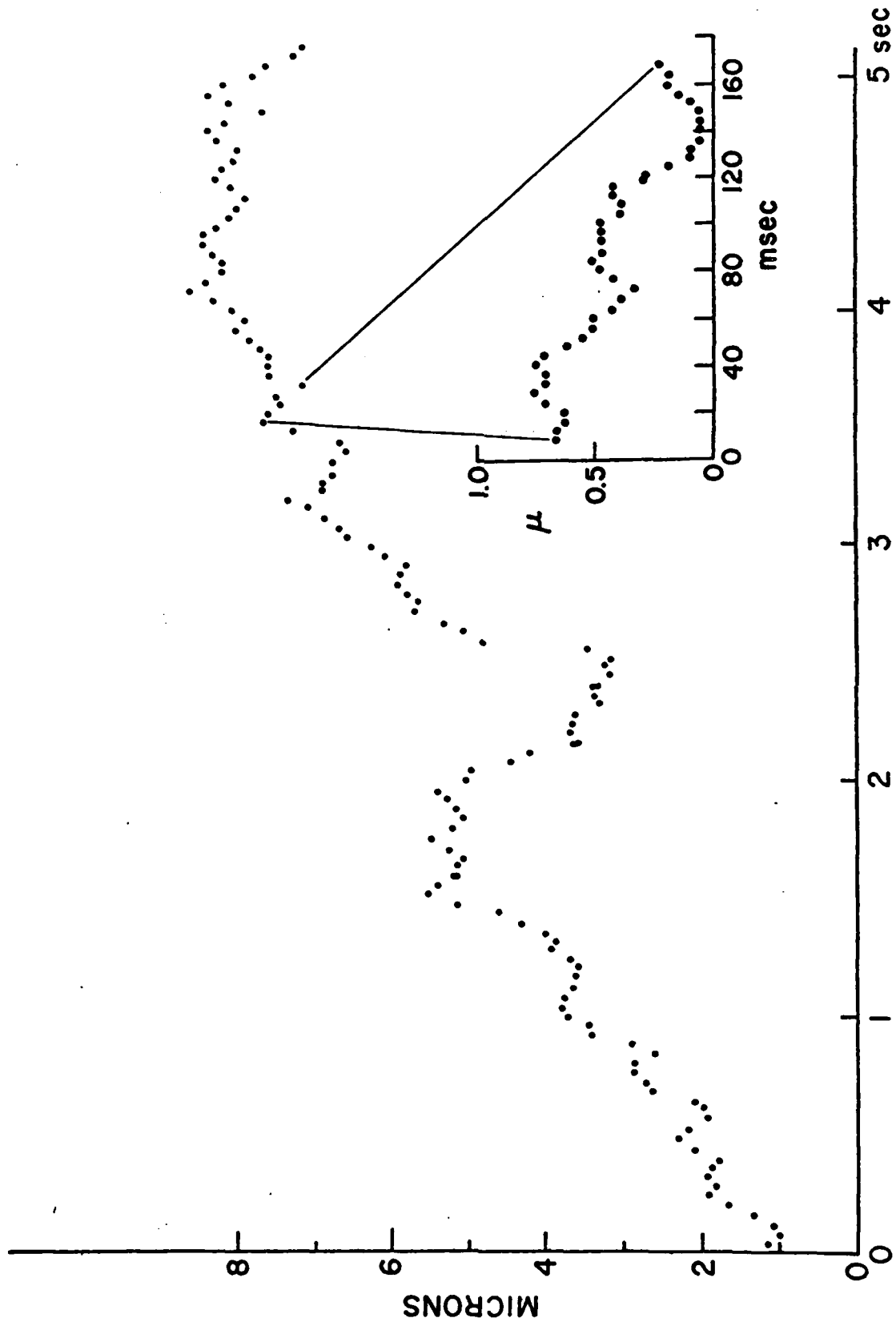




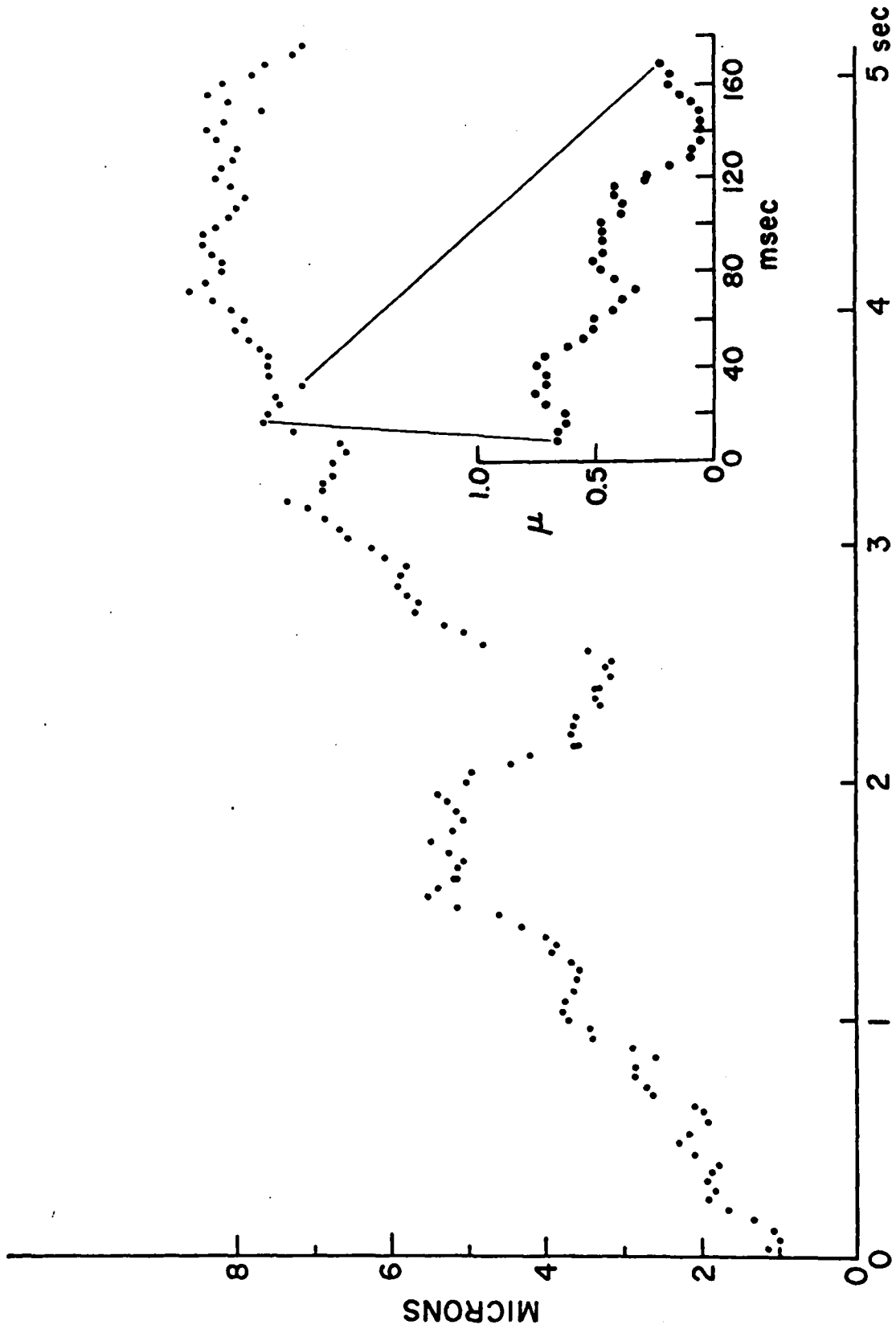
Handwritten text, possibly a signature or name, written in a cursive style.

A vertical line of text, possibly a date or a reference number.

Multiple lines of handwritten text, possibly a list or a series of entries.

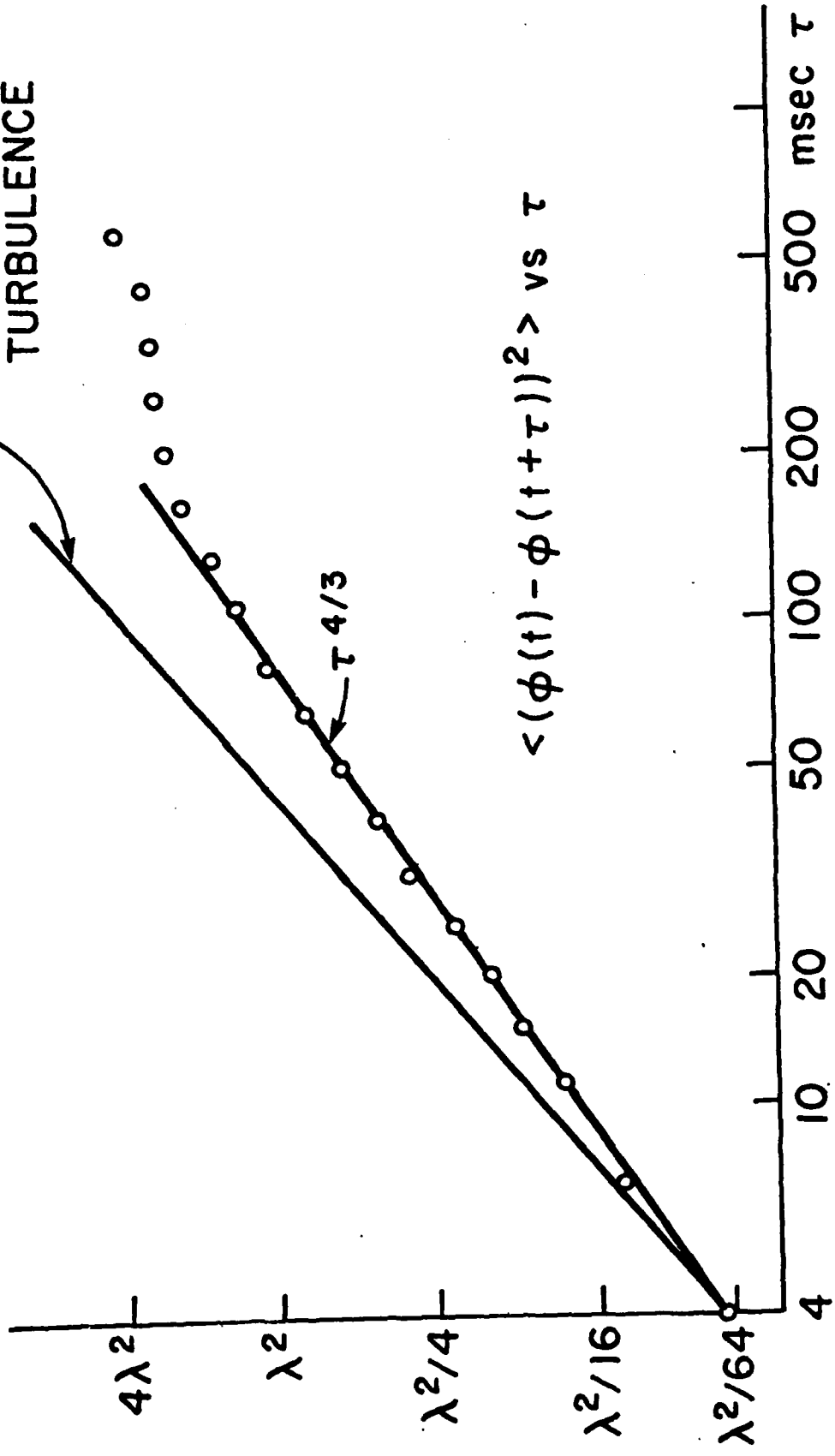


FRINGE MOTION DUE TO TURBULENCE AND EARTH ROTATION



FRINGE MOTION DUE TO TURBULENCE AND EARTH ROTATION

$\tau^{5/3}$ KOLMOGOROV
TURBULENCE



END

FILMED

1 84

DTIC